Current Biology 21, 278–287, February 22, 2011 ©2011 Elsevier Ltd All rights reserved DOI 10.1016/j.cub.2011.01.013

Article

Apoptosis Ensures Spacing Pattern Formation of *Drosophila* Sensory Organs

Akiko Koto,[1] Erina Kuranaga,[1,2,3] and Masayuki Miura[1,2,*]

[1]Department of Genetics, Graduate School of Pharmaceutical Sciences, University of Tokyo, 7-3-1 Hongo, Bunkyo-ku, Tokyo 113-0033, Japan

[2]Core Research for Evolutional Science and Technology (CREST), Japan Science and Technology Agency, 7-3-1 Hongo, Bunkyo-ku, Tokyo 113-0033, Japan

[3]Laboratory for Histogenetic Dynamics, RIKEN Center for Developmental Biology, 2-2-3 Minatojima-minamimachi, Chuo-ku, Kobe 650-0047, Japan

Summary

Background: In both vertebrates and invertebrates, developing organs and tissues must be precisely patterned. One patterning mechanism is Notch/Delta-mediated lateral inhibition. Through the process of lateral inhibition, *Drosophila* sensory organ precursors (SOPs) are selected and sensory bristles form into a regular pattern. SOP cell fate is determined by high Delta expression and following expression of neurogenic genes like *neuralized*. SOP selection is spatially and temporally regulated; however, the dynamic process of precise pattern formation is not clearly understood.

Results: In this study, using live-imaging analysis, we show that the appearance of *neuralized*-positive cells is random in both timing and position. Excess *neuralized*-positive cells are produced by developmental errors at several steps preceding and accompanying lateral inhibition. About 20% of the *neuralized*-positive cells show aberrant cell characteristics and high Notch activation, which not only suppress neural differentiation but also induce caspase-dependent cell death. These cells never develop into sensory organs, nor do they disturb bristle patterning.

Conclusions: Our study reveals the incidence of developmental errors that produce excess *neuralized*-positive cells during sensory organ development. Notch activation in *neuralized*-positive cells determines aberrant cell fate and typically induces caspase-dependent cell death. Apoptosis is utilized as a mechanism to remove cells that start neural differentiation at aberrant positions and timing and to ensure robust spacing pattern formation.

Introduction

Robust pattern formation in animal development requires accurately regulated cell fate determination, resulting in an adequate number of cells at proper positions at the right developmental timing. When the integrity of cell fate determination is disturbed, excess or aberrantly differentiated cells are produced, resulting in developmental defects and pathological conditions. If patterns are to form correctly, animals must promptly eliminate these aberrant cells. It has been shown that aberrant cells ectopically produced by genetic manipulation are eliminated by programmed cell death [1–6], suggesting that developing animals are innately equipped with fail-safe mechanisms that recognize and eliminate aberrant cells. However, the role of these fail-safe mechanisms in the context of normal development is not well described.

Programmed cell death plays an essential role in normal development. Massive cell death is observed in early neural development [7–9]. If cell death is inhibited, severe morphological defects are induced in the nervous system [10–16]. This indicates that during early neural development, proper neural tissue formation requires the death of a portion of the cells. However, the role of programmed cell death in the process of neural pattern formation is still obscure. The developmental timing, position, and differentiation state of dying cells have not been clearly defined as a result of the technical difficulties of tracing these cells in fixed tissue. Because aberrant cells are transient, it is difficult to determine the incidence of developmental errors in a dynamic developmental context. Thus, it has not been clear whether programmed cell death is linked to a fail-safe mechanism eliminating ill-defined cells in the process of neural pattern formation. Here, we examined (1) when, where, and how frequently aberrant cells are produced in normal development and (2) which fail-safe mechanisms are innately present to overcome the appearance of aberrant cells. Using live-imaging techniques, we could trace the dynamic developmental process through cell fate determination, differentiation, and death at single-cell resolution in living animals, providing new insight into the intrinsic fail-safe mechanisms for robust pattern formation.

The sensory organs on a fly's thorax, composed of large (macrochaetes) and small (microchaetes) bristles, are a well-known model of a robust spacing pattern (Figure 1A). In this study, we focused on microchaete development because this developmental process can be visualized with time-lapse imaging [17] and because the molecular mechanisms that produce the microchaete patterns have been well studied [18–21]. Previous studies showed that cell fate choice between sensory organ precursors (SOPs) and epithelial cells is rigidly determined by Notch/Delta-mediated lateral inhibition. It has also been suggested that developmental errors may be part of the process of SOP selection. For instance, during macrochaete development, multiple precursors are observed at the onset of SOP selection, whereas only one sensory organ develops from a single precursor cluster [22]. However, it remains obscure when, where, and how frequently developmental errors produce aberrant cells, or which mechanisms are involved in repairing the missteps in cell fate determination and eventually forming a robust sensory organ pattern.

In following the entire process of sensory organ formation, we found that *neuralized*-positive cells are not precisely patterned at the onset of SOP selection. At this early stage of SOP development, excess *neuralized*-positive cells appear at random positions and times. About 20% of the *neuralized*-positive cells display an intermediate character between SOP and epithelial cells, along with Notch activation; these cells do not develop into sensory organs. In these aberrantly differentiated cells, Notch activation induces not only the suppression of neural differentiation but also the execution of apoptosis. Notch-dependent fail-safe mechanisms are

*Correspondence: miura@mol.f.u-tokyo.ac.jp

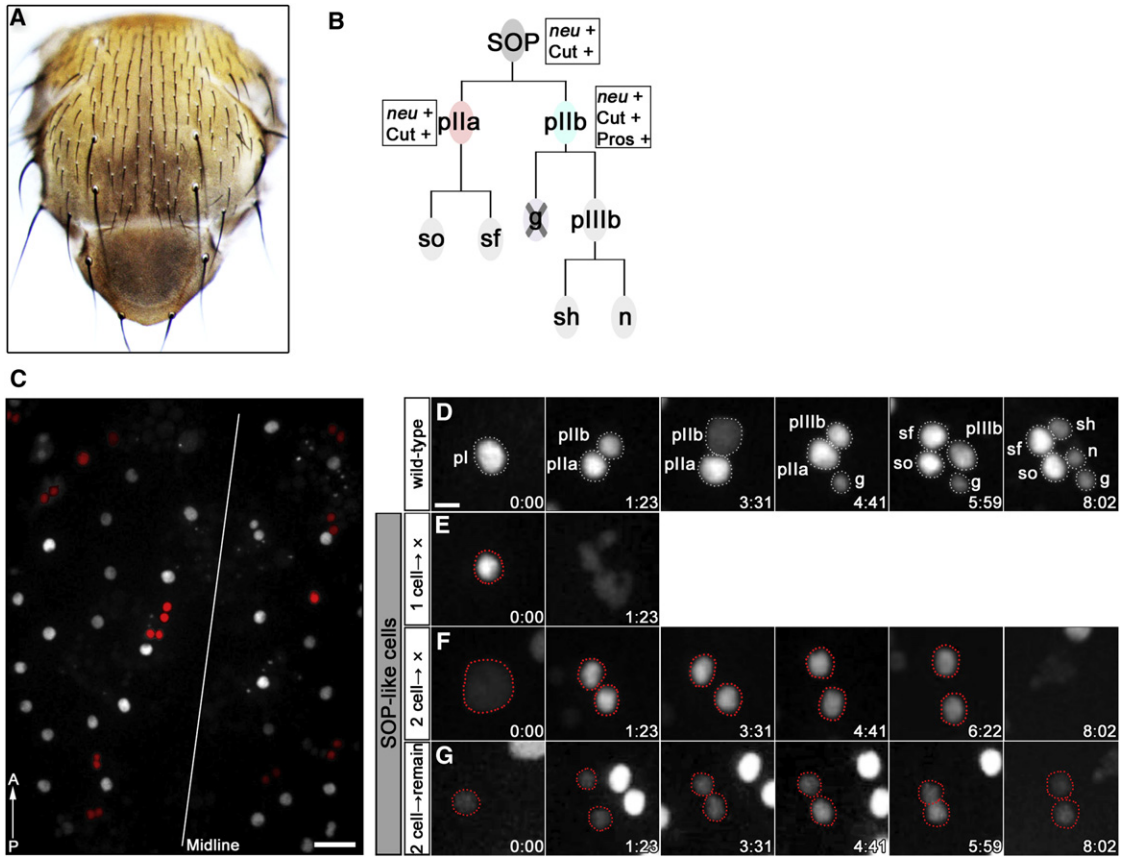

Figure 1. Some *neuralized*-Positive Cells Fail to Develop into Sensory Organs

(A) Light-microscopy image of sensory bristles on the notum region of a wild-type fly.

(B) The sensory organ precursor (SOP) lineage. The progenitor cells SOP, pIIa, pIIb, and pIIIb divide to form the five cells of the sensory organ. The lineage markers *neuralized* (*neu*), Cut, and Prospero (Pros) are seen to the side of SOP, pIIa, and pIIb.

(C–G) Confocal imaging of nuclear-localized Venus using a *neu-GAL4* driver.

(C) Positions of *neuralized*-positive cells in control flies. SOP-like cells are marked in red. Scale bar represents 20 μm.

(D–G) Snapshots at progressive stages of development. Scale bar in (D) represents 5 μm.

(D) An SOP shows four rounds of asymmetric cell division. The SOP and its progeny are outlined with white dotted lines.

(E) SOP-like cells disappearing at the one-cell stage.

(F) SOP-like cells disappearing at the two-cell stage.

(G) SOP-like cells remaining at the two-cell stage without subsequent cell division. The SOP-like cells are outlined with red dotted lines.

Genotypes shown are w^{1118} (A) and *UAS-nlsSCAT3/CyO;neu-GAL4/MKRS* (C–G).

utilized to eliminate the cells that begin neural differentiation at aberrant positions and times, and to promote the proper spatial pattern of bristles during development.

Results

Excess *neuralized*-Positive Cells Appear at the Onset of SOP Selection

During microchaete development, SOPs appear from the stripe regions of proneural cells expressing the proneural gene *achaete-scute* [23]. The SOPs begin expressing high Delta, which promotes Notch signaling activation to inhibit neural differentiation in the surrounding cells [24]. SOPs are marked by the expression of *neuralized*, which is expressed in SOPs as soon as they start to differentiate but is not expressed in epithelial cells [22, 25]. Time-lapse imaging of SOPs expressing nuclear-localized fluorescent protein in living pupae was performed with the *neuralized-GAL4* (*neu-GAL4*) driver [26], a GAL4 enhancer trap line in the *neu* locus that drives expression in the SOP lineage. Live imaging of SOPs began at the one- or two-cell stage at around 15 hr after puparium formation (APF) (Figure 1C; see also Movie S1 available online) and continued through their development into four cell types—socket, shaft, sheath, and neuron—after four rounds of asymmetric cell division (Figures 1B and 1D) [17, 27]. SOPs emerged asynchronously [25], and most of them developed into sensory organs.

However, we found that the *neuralized*-positive cells were not precisely spaced at the onset of SOP selection, which began at around 15 hr APF. We also observed that the fate of some *neuralized*-positive cells was completely different from that of other SOPs (compare Figures 1E–1G with Figure 1D). Their cell fates could be categorized in three types: disappearance at the one-cell stage (Figure 1E), disappearance at the two-cell stage (Figure 1F), and persisting at the two-cell stage without subsequent cell division (Figure 1G). These cells never differentiated into sensory organs, whereas normal SOPs (referred to hereafter simply as SOPs) finished a fourth round of cell division within 10 hr and developed normally into sensory organs. Therefore, we hereafter refer

to these aberrant cells that express *neuralized* but never develop into sensory organs as SOP-like cells.

SOP-like cells appeared both a few cells away and right next to SOPs (Figure 1C). These results indicate that at the first stage of SOP cell fate determination, the positions of the *neuralized*-positive cells are not precisely patterned, and that some *neuralized*-positive cells cannot develop into sensory organs.

Neural Differentiation of SOP-like Cells Stops at the One-Cell Stage

We next characterized the SOP-like cells using other SOP markers. The protein Cut, which localizes to the nuclei of all SOPs and their progeny cells (Figure 1B) [28], was expressed by the majority of the *neuralized*-positive cells at 19 hr APF at the two-cell stage. Some *neuralized*-positive cells without Cut were observed in close proximity to those expressing Cut (Figures 2A and 2A′). At 20–22 hr APF, SOPs developed to the three-cell stage, but SOP-like cells remained at the two-cell stage, without Cut protein (Figures 2B and 2B′). Prospero is expressed in the SOP-derived pIIb, glial, and sheath cells (Figure 1B) [17, 29, 30]. Prospero-negative SOP-like cells remained at the two-cell stage even at 20–22 hr APF (Figures 2C–2D′). Senseless was also not expressed in SOP-like cells at the two-cell stage (data not shown). Thus, SOP-like cells do not express the SOP markers Cut, Prospero, or Senseless, suggesting that their development as SOPs stopped at the one-cell or early two-cell stage after *neuralized* expression.

We next asked at what point *neuralized* is no longer expressed in SOP-like cells. We examined *neuralized* promoter activity by performing photobleaching in flies expressing histone 2B-ECFP via the *neu-GAL4* driver. SOPs recovered ECFP fluorescence after the photobleaching treatment, but SOP-like cells at the two-cell stage did not (Figures 2E and 2F), indicating that *neuralized* promoter activity had stopped by this stage. These results suggested that by amplifying *neuralized* expression with a GAL4 enhancer, we could trace the transient cell fate of SOP-like cells over long periods of live-imaging analysis. Furthermore, the distribution of Partner of numb (Pon)-GFP [31] indicated that the SOP-like cells divided symmetrically (Figure 2H), whereas SOPs showed an asymmetric distribution of Pon-GFP to pIIb cells (Figure 2G). In summary, SOP-like cells expressed *neuralized* but had stopped undergoing neural differentiation at the one-cell stage. To determine the SOP differentiation state at an earlier stage, we examined *Delta* expression using a *Delta-lacZ* reporter, and we found that the *Delta-lacZ* signal in the SOP-like cells was higher than that in the surrounding epithelial cells (Figure S1). This finding suggests that SOP-like cells express *Delta* at the beginning of their neural fate determination and that they have neural cell characteristics at early one-cell stage.

Caspase-Dependent Cell Death Eliminates Aberrant SOP-like Cells

About 20% of *neuralized*-positive cells were categorized as SOP-like cells (Figure 3A). As we followed cell development, we found that the great majority of SOP-like cells disappeared at the two-cell stage (Figure 1F; Figure 3B). To test whether caspase-dependent cell death was responsible for the disappearance of these SOP-like cells, we examined the activation of caspases over time with SCAT3, a fluorescence resonance energy transfer (FRET) indicator for effector caspase activity [32, 33]. A large majority (76%) of SOP-like cells showed high caspase activation preceding nuclear fragmentation and death at two-cell stage (Figure 3C; Figure S2B). The decrease in FRET of SCAT3 was observed within 15 min before nuclear fragmentation in dying SOP-like cells at the one-cell and two-cell stage (Figures S2A, S2B, and S2D). On the other hand, persisting SOP-like cells (Figures S2C and S2D) and cells in the SOP lineage except for glial cells [34, 35] did not show caspase activation. Furthermore, epithelial cells rarely disappeared during SOP development from 15 to 27 hr APF, except in the midline region where the contralateral discs fuse together [36] (Figures S2E and S2F), suggesting that caspase activation is specifically induced in SOP-like cells in pupal nota during sensory organ formation.

To determine whether caspase functions to eliminate SOP-like cells, we performed live imaging of SOP development in flies expressing the caspase inhibitor p35 with *neu-GAL4*. The percentage of SOP-like cells in the p35-expressing flies was almost the same as in the controls (Figure 3A). However, their cell fate changed; most of the SOP-like cells did not disappear but remained at the two-cell stage (Figure 1G; Figure 3B; Movie S2), indicating that when caspase is not inhibited, the majority of SOP-like cells undergo cell death accompanied by caspase activation. We next examined the involvement of the proapoptotic genes *reaper*, *hid*, and *grim* (*RHG*) in SOP-like cells' death. Results similar to those found with the p35-expressing flies were observed following *neu-GAL4*-induced expression of *UAS-RHG microRNA* (*RHG* miRNA) (Figures 3A and 3B) [37]. This indicates that caspase activation in SOP-like cells is induced via one or more of the proapoptotic regulators *reaper*, *hid*, or *grim*.

Intriguingly, in the absence of the cell death pathway, the bristle pattern was not disturbed in adult flies, and the remaining SOP-like cells did not develop into ectopic sensory organs (Figures S2G–S2J). To test the possibility that persisting SOP-like cells differentiate into epithelial cells, we examined their nuclear position and the formation of epithelial junctions between surrounding cells. At the time when SOPs developed to the four-cell stage (Figure 3D), SOP-like cells at the two-cell stage were located in the monolayer epithelial sheet and formed normal junctions marked by E-cadherin expression with neighboring epithelial cells (red arrowheads in Figure 3E), suggesting that persisting SOP-like cells differentiate into epithelial cells. The remaining SOP-like cells in the p35-expressing flies also showed epithelial differentiation (data not shown).

Taken together, these results show that caspase-dependent cell death functions to specifically remove SOP-like cells. Even if caspase activation is blocked, the SOP-like cells do not develop into sensory organs; instead, they adopt an alternate fate, becoming epithelial cells and thereby supporting the robust patterning of the bristles.

Birth Timing Does Not Determine the Aberrant Cell Fate of SOP-like Cells

We next investigated the mechanisms determining the fate of SOP-like cells and asked whether the birth order of SOPs determined whether they became SOP-like cells at the onset of SOP selection. It is known that SOPs inhibit neighboring cells from differentiating into SOPs via Notch/Delta-mediated lateral inhibition [24]. We therefore examined whether the fate of SOP-like cells was determined by lateral inhibition from preceding SOPs, as in the case of the surrounding epithelial cells. If this were correct, all of the SOP-like cells would appear after already-existing SOPs. Contrary to our

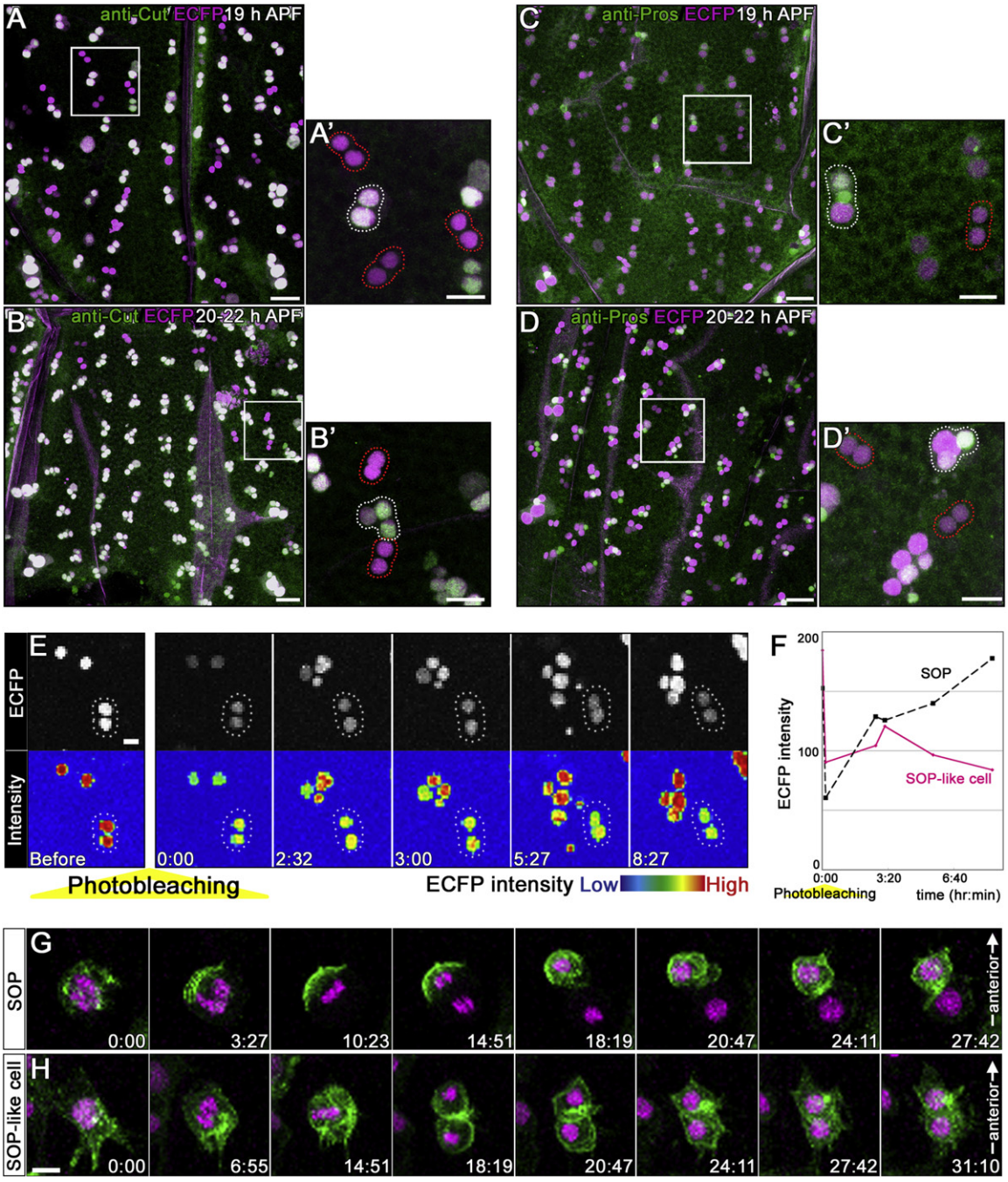

Figure 2. Aberrant Cell Characteristics in Ectopically Appearing SOP-like Cells

(A–D) SOP-like cells do not express SOP lineage markers except for *neuralized*. Immunostaining with anti-Cut (A and B, green) or anti-Prospero (C and D, green) antibodies at 19 hr after puparium formation (APF) (A and C) and 20–22 hr APF (B and D) is shown. *neuralized*-positive cells are marked using histone 2B-ECFP (magenta). Scale bars represent 20 μm.

(A′–D′) Magnified images of the boxed regions in (A)–(D). SOPs are marked by white dotted lines and SOP-like cells by red dotted lines. Scale bars represent 10 μm.

(E and F) *neuralized* promotor activity stops in SOP-like cells at the two-cell stage.

(E) ECFP fluorescence did not recover in SOP-like cells (white dotted line) but recovered in adjacent SOPs after ECFP photobleaching treatment. Scale bar represents 5 μm.

(F) Sequential variations of ECFP intensity in SOP (black dotted line) and SOP-like (magenta line) cells.

(G and H) Pon-GFP is localized asymmetrically in SOPs (G) but symmetrically in SOP-like cells during the first cell division (H). Scale bar in (H) represents 5 μm.

Genotypes shown are *neu-GAL4 UAS-Histone2B-ECFP/TM6B* (A-E) and *UAS-Histone2B-ECFP/+;neur^{P72}-GAL4 UAS-ponGFP/+* (G and H).

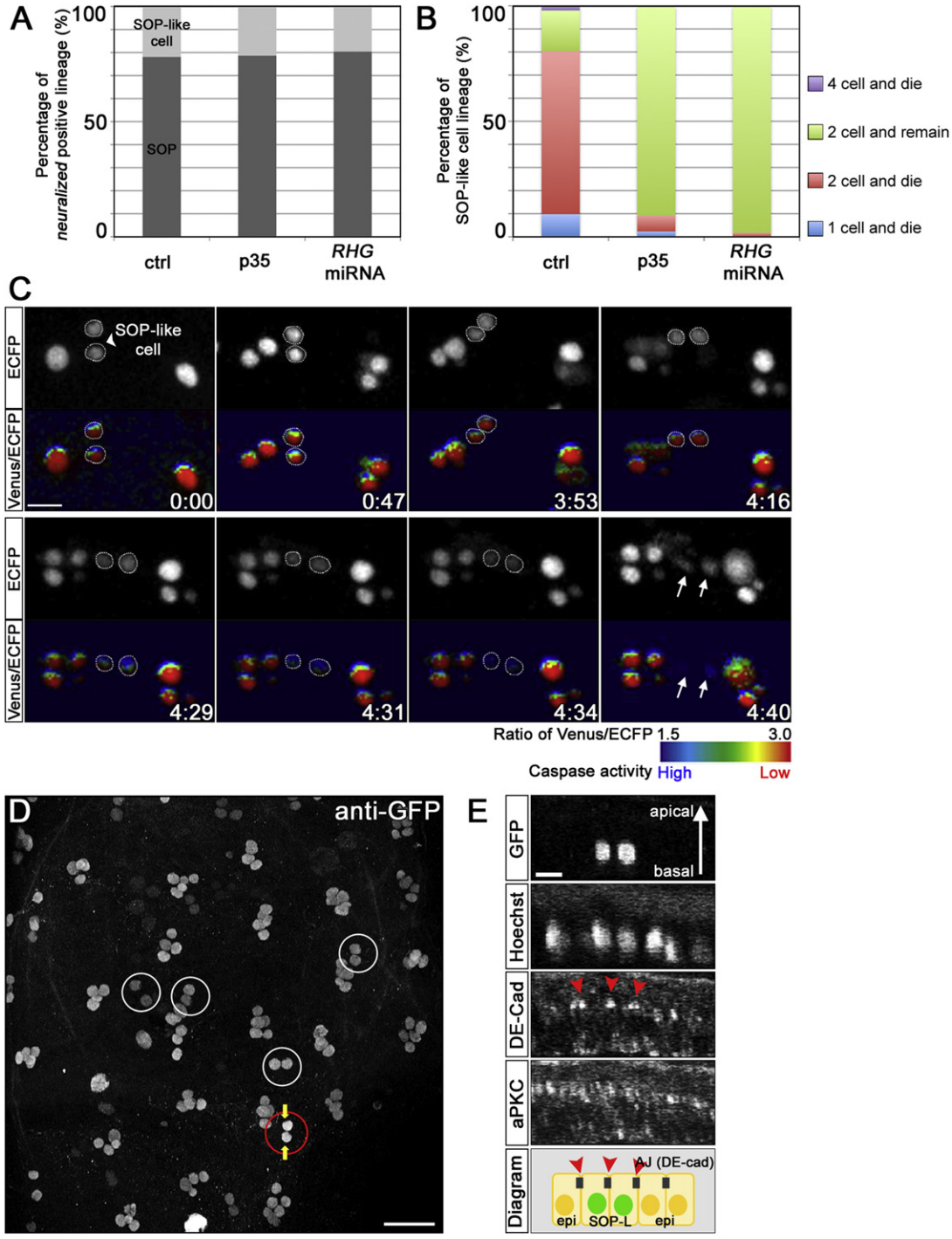

Figure 3. Caspase-Dependent Death of SOP-like Cells

(A) Proportion of SOPs and SOP-like cells in control (n = 234), p35- (n = 202), and *RHG* miRNA-expressing (n = 282) lineages. About 20% of *neuralized*-positive cells do not progress to sensory organs.

(B) Final cell fate of SOP-like cells in control, p35-, and *RHG* miRNA-expressing lineages.

(C) Caspase activation was detected in SOP-like cells (white dotted lines) prior to nuclear fragmentation (arrows). The lower row of panels show caspase activity images taken with a FRET-based probe, nls-SCAT3, and shown in pseudocolor. Scale bar represents 10 μm.

(D) Positions of *neuralized*-positive cells marked by an anti-GFP antibody at 21–25 hr APF. Most SOPs developed to the four-cell stage, whereas SOP-like cells (white and red circles) remained at the two-cell stage. Scale bar represents 20 μm.

(E) Single z section of an SOP-like cell (red circle in D). Yellow arrows in (D) indicate the cross-section direction. Persisting SOP-like cells were located in the monoepithelial layer and formed adherens junctions (red arrowheads) with surrounding epithelial cells. A schematic representation of an adherens junction (AJ), depicted in gray, between SOP-like cells (SOP-L) and epithelial cells (epi) is shown at the bottom. Scale bar represents 5 μm.

Genotypes shown are *UAS-nlsSCAT3/CyO;neu-GAL4/MKRS* (control in A–C), *UAS-nlsSCAT3/UAS-p35;neu-GAL4/UAS-p35* (p35 in A and B), *UAS-nlsSCAT3/UAS-RHG miRNA;neu-GAL4/+*(*RHG* miRNA in A and B), and *neu-GAL4 UAS-Histone2B-ECFP/TM6B* (D and E).

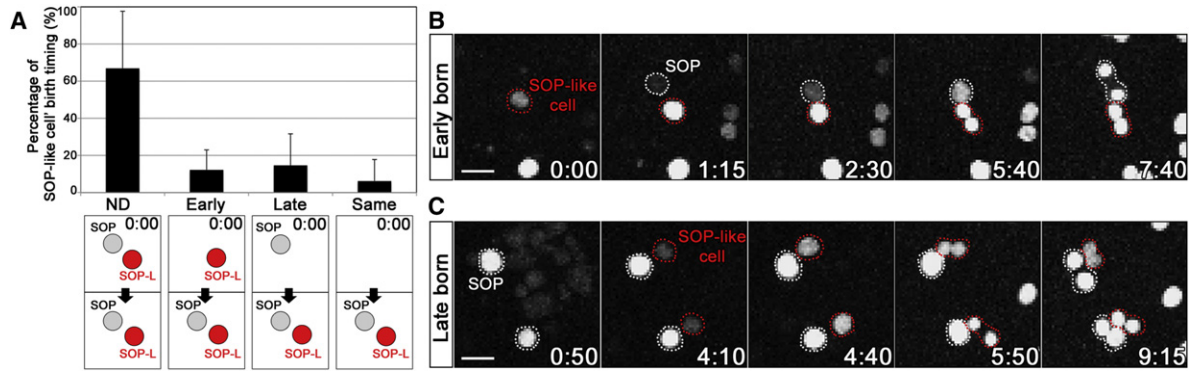

Figure 4. Birth Order of SOPs and SOP-like Cells Is Random

Birth timing of SOP-like cells (SOP-L) compared with adjacent SOPs (A; mean ± standard deviation, n = 5). "ND" indicates that both SOP and SOP-like cells already existed when live imaging started. "Early" indicates cases where an SOP-like cell (red) appeared first and an SOP (gray) appeared later, as shown in (B). "Late" indicates cases where an SOP preceded an SOP-like cell, as shown in (C). SOPs are indicated by white dotted lines; SOP-like cells are indicated by red dotted lines. Scale bars represent 10 μm. Genotype shown is *neu-GAL4 UAS-Histone2B-ECFP/TM6B*.

expectation, we found that the birth order of SOPs and SOP-like cells was random; not all SOP-like cells were born after the adjacent SOPs (Figure 4). Because SOP development starts just before pupal head eversion, the majority of SOPs and SOP-like cells were already present when time-lapse imaging started (around 15 hr APF), and these cases were categorized as ND (no data) in Figure 4A.

At the onset of SOP selection, the appearance of *neuralized*-positive cells did not follow a pattern in either birth position or timing, suggesting that the fate of SOP-like cells is not necessarily dictated by lateral inhibition from SOPs. However, SOP-like cells appearing later (Figure 4C) may be determined by lateral inhibition. This observation supports the model recently proposed by Barad et al. [38] and Cohen et al. [39], who showed that even when SOP-like cells appear ectopically, they cannot differentiate into sensory organs because of Notch/Delta-mediated lateral inhibition via *cis*-interaction or filopodia-mediated signal transduction. On the other hand, we found that a portion of SOP-like cells appeared earlier than the adjacent SOPs (Figure 4B), which is not consistent with lateral inhibition. This indicates that the SOP-like cells are not predetermined by birth timing.

Notch Determines the Cell Fate of SOP-like Cells at the Onset of SOP Selection

To examine the mechanisms determining the fate of SOPs and SOP-like cells, we next studied the functions of Notch signaling in three ways. We first examined the spatiotemporal pattern of Notch activation in SOP-like cells using the Notch activity marker *Enhancer of split mα-GFP* [*E(spl)mα-GFP*] [40, 41]. The high stability of GFP protein makes it difficult to detect the state of Notch activation simply by calculating GFP intensity, so to monitor the Notch activation level more precisely, we used photobleaching to examine the promoter activity of *E(spl)mα*. Photobleaching was performed at the one-cell stage when *neu-GAL4* expression had just started, as indicated by low ECFP intensity (Figures 5B and 5D). In SOPs, the GFP recovery rate after photobleaching was low (Figures 5A and 5B). On the other hand, the GFP fluorescence recovered to a high intensity in SOP-like cells (Figures 5C and 5D). The recovery rates varied by cell lineage, but the average rate in SOP-like cells was remarkably higher than that in SOPs (thick green lines in Figures 5B and 5D). The high GFP recovery was detected in SOP-like cells regardless of whether they were adjacent to SOPs (Figures S3A and S3B). These results suggest that Notch activity persists in SOP-like cells at the one-cell stage, but not in SOPs.

Next, to investigate the effect of Notch signaling on the cell fate of SOP-like cells, we used live imaging to determine the frequency of SOP-like cells in flies in which Notch signaling was manipulated. *Notch^{55e11}* is the null allele of *Notch*; its heterozygous mutant shows an increased bristle phenotype in adult flies [42, 43]. If Notch signaling determines the cell fate of SOPs and SOP-like cells, the appearance ratio of SOP-like cells to SOPs would change in the *N^{55e11}* heterozygous mutant. We traced the cell fate of each *neu-GAL4*-positive lineage in the *N^{55e11}* heterozygous mutant and found that the proportion of SOP-like cells was dramatically reduced in flies with an *N^{55e11}* heterozygous background (Figure 5E; Figure S3C; Movie S3). Although it could not be definitely stated that the increase in SOPs in the *N^{55e11}*/+ mutant corresponded to the SOP-like cells observed in controls, we found that the increase in the number of bristles in *N^{55e11}*/+ mutant flies nearly coincided with the number of SOP-like cells observed in controls. In controls, about 20% of the *neuralized*-positive cells were categorized as SOP-like cells (Figure 5E). In *N^{55e11}* heterozygous mutant flies, the final bristle number was increased by about 20% as compared to control flies (Figures S3D–S3F). These results suggest that Notch signaling contributes to determining a certain portion of SOPs to be SOP-like cells.

Finally, to examine the involvement of SOPs in the cell fate determination of SOP-like cells, we traced the fate of SOP-like cells after adjacent SOPs had been removed (Figure 5F; Movie S4). SOP ablation was performed with multiphoton laser microscopy when both the SOPs and the surrounding SOP-like cells were at the one-cell stage, because SOP-like cells lose their neural cell character at the one-cell stage (Figure 2). By comparing the *E(spl)mα-GFP* intensity, we could identify the cells predicted to become SOPs or SOP-like cells at the one-cell stage. The SOP with the lowest GFP intensity among three adjacent *neuralized*-positive cells (red cell indicated by arrowheads in Figure 5F) was ablated, and its death was confirmed by its nuclear fragmentation (arrowheads at time 0:00 in Figure 5F). Two SOP-like cells (cells colored yellow and aqua in Figure 5F) started to divide after the adjacent

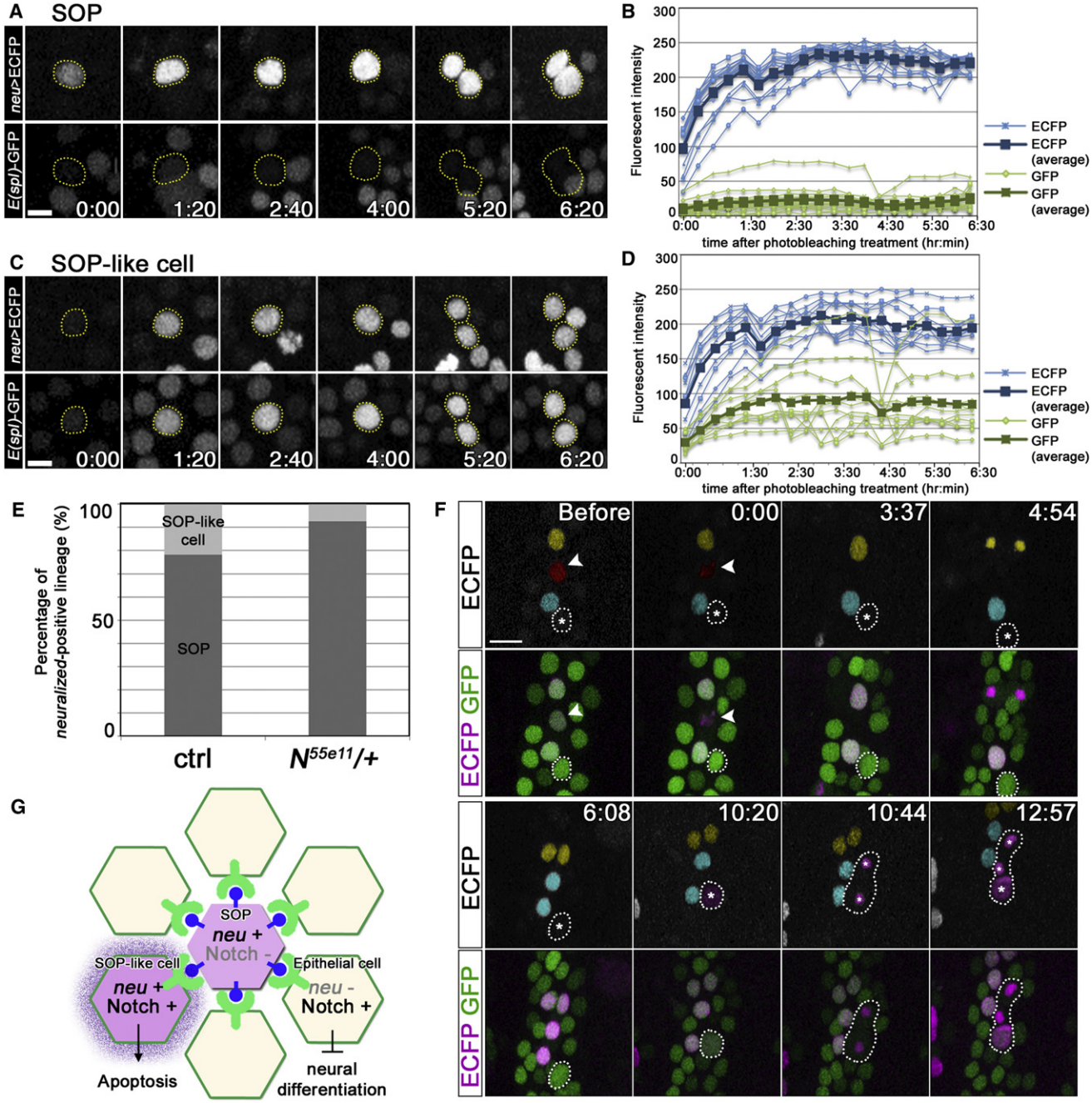

Figure 5. Notch Signaling Affects Cell Fate Determination of SOP-like Cells

(A–D) Notch activity persists in SOP-like cells, but not in SOPs, after *neuralized* expression. We used an *E(spl)mα-GFP* reporter to measure GFP fluorescence recovery after photobleaching treatment at the one-cell stage in SOPs (A and B) and SOP-like cells (C and D).

(A and C) ECFP and GFP fluorescent signals at progressive stages after photobleaching in an SOP (A) and an SOP-like cell (C). Scale bars represent 5 μm.

(B and D) Sequential variations in GFP (green) and ECFP (blue) fluorescence intensity in SOPs (B; n = 14) and SOP-like cells (D; n = 11). Thick lines indicate the average of each fluorescence.

(E) The proportion of SOPs and SOP-like cells in N^{55e11}/+ flies (n = 491).

(F) SOP-like cells (two cell lineages colored yellow and aqua) do not develop into sensory organs even when an adjacent SOP is ablated (red cell indicated by arrowhead) (n = 6). An alternate SOP appears from an epithelial cell (outlined by white dotted lines, with asterisks). To trace each cell lineage, four independent lineages are shown in pseudocolor (ablated SOP, red; SOP-like cells, yellow and aqua; late-appearing SOP, pink) in the upper row of panels (ECFP). In the lower row of panels, merged images of ECFP (magenta) and GFP (green) are shown. Scale bar represents 10 μm.

(G) SOP-like cells expressing *neuralized* (*neu* +; colored in pink) and exhibiting persistent Notch activation (Notch +; outlined in green) die with caspase activation. SOP cells (*neu* +, Notch −) suppress neural differentiation in surrounding epithelial cells (*neu* −, Notch +).

Genotypes shown are *E(spl)mα-GFP/+;neu-GAL4 UAS-Histone2B-ECFP/+* (A–D and F), *UAS-nlsSCAT3/CyO;neu-GAL4/MKRS* (control in E), and N^{55e11} *FRT19A/+;UAS-nlsSCAT3/+;neu-GAL4/+* (N^{55e11}/+ in E).

SOP's death but never entered the next cell cycle or developed into sensory organs. Instead, one nearby epithelial cell (indicated by white dotted lines and asterisks in Figure 5F), which had been two cells away from the ablated SOPs, started to express *neu-GAL4* (from time 10:20 in Figure 5F) and finally developed into a sensory organ after four rounds of cell division. The appearance of an alternative SOP indicates that ablating incipient SOPs unlocks Notch/Delta-mediated lateral inhibition, after which surrounding epithelial cells have the plastic property to develop into SOPs. It is noteworthy that even when the Notch/Delta-mediated lateral inhibition was removed, the adjacent SOP-like cells did not have the ability to differentiate into SOPs. Taking these findings together, Notch activation in an SOP determines its fate as an SOP-like cell (Figure 5G), and once Notch is highly activated in an early stage of neural differentiation, its fate as an SOP-like cell is irreversible. Notch activation drives two backup systems to eliminate these aberrant SOP-like cells in animals: one is the suppression of neural differentiation, and the other is the execution of caspase-dependent cell death.

Discussion

The *Drosophila* sensory organ is a typical model for the study of Notch/Delta-mediated lateral inhibition. The mechanisms of its pattern formation have been studied over long periods by analyzing various mutants [24, 44, 45]. Although sensory organs develop spatially and temporally [25], the sequential process of pattern formation has not been described in detail. Tracking the process of cell fate determination in each cell lineage is presumed to be effective in revealing the mechanisms behind precise pattern formation.

Our first finding in this study is that bristle patterning starts in a random fashion, which is consistent with recently reported results [39] in the following two regards: about 20% of *neuralized*-positive cells are fated to become aberrant SOP-like cells (Figure 3A), and Notch signaling is involved in determining the fate of SOP-like cells (Figure 5). However, the mechanisms proposed for the production of SOP-like cells in the above-mentioned report do not coincide perfectly with our observations. Previous studies showed that the conventional model of Notch/Delta-mediated lateral inhibition is not sufficient to produce the precise bristle pattern but that cell-autonomous interaction [38] or filopodia-mediated intermittent Notch/Delta signaling [39] makes lateral inhibition robust enough to suppress the neural differentiation of surrounding cells. In contrast, our results suggest that lateral inhibition from adjacent SOPs is not the sole source of Notch activation in SOP-like cells, because a portion of SOP-like cells preceded the nearby SOPs, as shown in Figure 4. Also, SOP-like cells showed ongoing Notch activity even in the absence of adjacent SOPs (Figure S3B). One possible explanation for these SOP-like cells failing to develop into sensory organs may be that they appear too early in the developmental time course and cannot complete the developmental program to become sensory organs in a cell-autonomous manner. In any case, the decrease in SOP-like cells in the N^{55e11} heterozygous mutant reliably suggests that Notch activation in cells that start neural differentiation contributes to the determination of their cell fate as aberrant SOP-like cells.

Dynamic oscillation of the Notch effector gene *Hes1* has been observed in neural progenitors of the developing mouse brain [46, 47] with the aid of a short-half-life indicator using ubiquitinated firefly luciferase [47, 48]. In *Drosophila* sensory organ development, the technical limitations of the GFP reporter make it difficult to confirm this type of oscillation pattern in Notch signaling (Figures 5A–5D). However, given that Notch oscillation occurs in cells in the proneural stripe regions at the beginning of SOP selection, it is conceivable that SOP-like cells might be the product of fluctuating Notch signaling at inappropriate times, developmentally speaking.

Our second finding in this study is that a program of caspase-dependent cell death specifically eliminates SOP-like cells. We showed that ablating an incipient SOP removes Notch/Delta-mediated lateral inhibition and allows a nearby epithelial cell to become the SOP, as has also been observed in the embryonic central nervous system of grasshoppers [49]. However, the adjacent SOP-like cells never develop into sensory organs, suggesting that the fate of SOP-like cells is irreversible (Figure 5F). By observing the nuclear morphology along with an indicator for caspase activation, we noted that in the process of sensory organ development, only SOP-like cells showed the typical features of programmed cell death (Figure 3C). These results indicate that programmed cell death ensures robust pattern formation by eliminating aberrantly differentiated cells.

The significance of programmed cell death in pattern formation has been well studied, especially in the development of the fly eye [50, 51]. Each ommatidium is composed of eight photoreceptor neurons and six support cells, consisting of four cone cells and two primary pigment cells. Between each ommatidium, remaining cells form the interommatidial lattice. Excess pigment cells are eliminated through programmed cell death. Notch functions within the interommatidial lattice to induce cell death, and the primary pigment cells send a survival signal to adjacent cells [52, 53]. The life-and-death fate of interommatidial cells is decided by their position and the cells to which they are attached. In the case of sensory organ formation, Notch signaling is crucial in determining the aberrant cell fate of SOP-like cells. However, Notch activation alone seems insufficient to induce programmed cell death, because the surrounding epithelial cells do not disappear, even though they exhibit high levels of Notch activation during sensory organ development (Figures S2E and S2F). Therefore, some factor that marks neural differentiation in SOP-like cells may be required to induce cell suicide. We found that ectopic *neuralized* expression did not induce the aberrant cell fate or cell death in epithelial cells (data not shown), suggesting that *neuralized* itself is not essential in determining the aberrant cell fate of SOP-like cells. Therefore, to determine how apoptosis is induced in SOP-like cells, we next examined the effect of Notch activation in *neuralized*-positive cells at the one-cell stage using the temporal and regional gene expression targeting (TARGET) system with *tub-GAL80^{ts}* (Figures S3G–S3K). As reported previously, activated Notch induced the multiple-sockets phenotype (Figure S3I) [54]. At the same time, about 50% of *neuralized*-positive cell lineages died, accompanied by nuclear fragmentation (Figure S3J; Movie S5), causing a dramatic bald phenotype that was observed in the adult flies (Figure S3I). These findings suggest that the combination of neural differentiation in the SOP lineage and Notch activation switches on cell death signaling. One possible future approach to searching for the killing factor expressed in SOP-like cells would be gene profiling using laser microdissection [55].

When the apoptotic pathway is blocked, the inhibition of cell death results in cell fate transformation [56, 57]. In *C. elegans*, cell death survivors in *ced-3* mutants exhibit an ambiguous cell

fate [58]. The most disruptive alternative cell fate occurs when the remaining cells differentiate into tumor-like proliferating cells, as shown in the development of the *Drosophila* serotonin lineage [59]. Under apoptosis-deficient conditions, other types of cell death occur, such as necrosis or autophagic cell death [37, 60, 61]. These alternate reactions could mask the incidence of programmed cell death; therefore, it is possible that the role of the apoptotic pathway has been missed in the case of sensory organ development. In this study, we showed that SOP-like cells differentiate into epithelial cells when the cell death pathway is blocked (Figure 3E). Time-lapse imaging made it possible to trace the transient fate of dying SOP-like cells, revealing the contribution of programmed cell death in the SOP selection process. Although the function of apoptosis has been emphasized in various developmental processes, the principle message is that several pathways exist to overcome the appearance of excess or aberrant cells and to make the developmental process more robust. Our study reveals that programmed cell death plays an important role in overcoming innately induced developmental errors and contributing to robust neural cell selection.

Experimental Procedures

Fly Strains

The following fly strains were used: *neu-GAL4* (Bloomington Drosophila Stock Center), *UAS-nlsSCAT3*, *UAS-Histone2B-ECFP* [35], *UAS-p35* [62], *UAS-RHG miRNA* [37], *yw;neur^{P72}-GAL4 UAS-PonGFP/TM6C* [31], *E(spl)mα-GFP* [41], and *Notch^{55e11}* [43].

Antibodies

The following antibodies and dilutions were used: mouse anti-Cut (Developmental Studies Hybridoma Bank [DSHB]), 1:20; mouse anti-Prospero (DSHB), 1:5; rabbit anti-aPKCζ (C-20, Santa Cruz), 1:500; rat anti-DCad2 (DSHB), 1:25; chicken anti-GFP (Aves Laboratories), 1:500; anti-chicken IgY FITC, 1:500; anti-rabbit IgG Cy5, 1:100; anti-rat IgG Cy3, 1:100; anti-mouse IgG Cy5, 1:100 (Jackson ImmunoResearch Laboratories).

Time-Lapse Recording

Sample preparation was performed as described previously [35]. Live imaging for FRET was performed on a Leica DM6000 B microscope equipped with a CSU10 confocal unit (Yokogawa) and a cooled charge-coupled device camera (CoolSNAP HQ; Photometrics, Roper) at 22°C using a Leica HCX PL 40× NA 1.25–0.75 oil-immersion objective lens. Image acquisition and analysis were performed using MetaMorph software (Molecular Devices), and Adobe Photoshop CS3 was used to adjust brightness and contrast. In most cases, the animal survived the data acquisition and developed into an adult.

Laser Ablation

Staged pupae were prepared as described previously [35]. SOPs were identified by ECFP expression via a *neu-GAL4* driver. An 840 nm wavelength laser beam was directed on the target SOP using a Leica HCX PL 63× NA 1.40–0.60 oil-immersion objective lens and 64× zoom factor. After the ablation treatment, time-lapse imaging was performed using a confocal subunit with a Leica HCX PL 40× NA 1.25–0.75 oil-immersion objective lens. Laser ablation and serial live imaging were performed on a Leica TCS SP5 multiphoton confocal microscope system.

Supplemental Information

Supplemental Information includes three figures, Supplemental Experimental Procedures, and five movies and can be found with this article online at doi:10.1016/j.cub.2011.01.015.

Acknowledgments

We thank J.W. Posakony, F. Schweisguth, B. Hay, C.-H. Chen, A.W. Moore, and H.J. Bellen for providing fly strains and materials and the Bloomington Drosophila Stock Center and the Drosophila Genetic Resource Center (Kyoto Institute of Technology, Kyoto, Japan) for providing fly strains. We are grateful to S. Hayashi for helpful discussions and encouragement, to H. Kanuka for kind support, and to T. Igaki for critical reading of the manuscript and helpful discussions. We thank T. Chihara and Y. Yamaguchi for helpful advice and critical reading of the manuscript. We thank the University of Tokyo and the Leica Microsystems Imaging Center (TLI) for imaging analysis. This work was supported by grants from the Japanese Ministry of Education, Culture, Sports, Science and Technology (to M.M. and E.K.), the Astellas Foundation for Metabolic Disorders (to M.M.), the Naito Foundation (to M.M. and E.K.), the Cell Science Research Foundation (to M.M.), a RIKEN Bioarchitect Research Grant (to M.M.), the Uehara Memorial Foundation (to E.K.), the Kanae Foundation for the Promotion of Medical Science (to E.K.), and the Takeda Science Foundation (to E.K.).

Received: October 1, 2010
Revised: December 3, 2010
Accepted: January 6, 2011
Published online: January 27, 2011

References

1. Adachi-Yamada, T., Fujimura-Kamada, K., Nishida, Y., and Matsumoto, K. (1999). Distortion of proximodistal information causes JNK-dependent apoptosis in Drosophila wing. Nature *400*, 166–169.
2. Brumby, A.M., and Richardson, H.E. (2003). scribble mutants cooperate with oncogenic Ras or Notch to cause neoplastic overgrowth in Drosophila. EMBO J. *22*, 5769–5779.
3. Herz, H.M., Chen, Z., Scherr, H., Lackey, M., Bolduc, C., and Bergmann, A. (2006). vps25 mosaics display non-autonomous cell survival and overgrowth, and autonomous apoptosis. Development *133*, 1871–1880.
4. Igaki, T., Pagliarini, R.A., and Xu, T. (2006). Loss of cell polarity drives tumor growth and invasion through JNK activation in Drosophila. Curr. Biol. *16*, 1139–1146.
5. Namba, R., Pazdera, T.M., Cerrone, R.L., and Minden, J.S. (1997). Drosophila embryonic pattern repair: how embryos respond to bicoid dosage alteration. Development *124*, 1393–1403.
6. Wu, M., Pastor-Pareja, J.C., and Xu, T. (2010). Interaction between Ras(V12) and scribbled clones induces tumour growth and invasion. Nature *463*, 545–548.
7. Buss, R.R., Sun, W., and Oppenheim, R.W. (2006). Adaptive roles of programmed cell death during nervous system development. Annu. Rev. Neurosci. *29*, 1–35.
8. de la Rosa, E.J., and de Pablo, F. (2000). Cell death in early neural development: Beyond the neurotrophic theory. Trends Neurosci. *23*, 454–458.
9. Kuan, C.Y., Roth, K.A., Flavell, R.A., and Rakic, P. (2000). Mechanisms of programmed cell death in the developing brain. Trends Neurosci. *23*, 291–297.
10. Cecconi, F., Alvarez-Bolado, G., Meyer, B.I., Roth, K.A., and Gruss, P. (1998). Apaf1 (CED-4 homolog) regulates programmed cell death in mammalian development. Cell *94*, 727–737.
11. Yoshida, H., Kong, Y.Y., Yoshida, R., Elia, A.J., Hakem, A., Hakem, R., Penninger, J.M., and Mak, T.W. (1998). Apaf1 is required for mitochondrial pathways of apoptosis and brain development. Cell *94*, 739–750.
12. Hakem, R., Hakem, A., Duncan, G.S., Henderson, J.T., Woo, M., Soengas, M.S., Elia, A., de la Pompa, J.L., Kagi, D., Khoo, W., et al. (1998). Differential requirement for caspase 9 in apoptotic pathways in vivo. Cell *94*, 339–352.
13. Kuida, K., Haydar, T.F., Kuan, C.Y., Gu, Y., Taya, C., Karasuyama, H., Su, M.S., Rakic, P., and Flavell, R.A. (1998). Reduced apoptosis and cytochrome c-mediated caspase activation in mice lacking caspase 9. Cell *94*, 325–337.
14. Kuida, K., Zheng, T.S., Na, S., Kuan, C., Yang, D., Karasuyama, H., Rakic, P., and Flavell, R.A. (1996). Decreased apoptosis in the brain and premature lethality in CPP32-deficient mice. Nature *384*, 368–372.
15. Abrams, J.M., White, K., Fessler, L.I., and Steller, H. (1993). Programmed cell death during Drosophila embryogenesis. Development *117*, 29–43.
16. White, K., Grether, M.E., Abrams, J.M., Young, L., Farrell, K., and Steller, H. (1994). Genetic control of programmed cell death in Drosophila. Science *264*, 677–683.
17. Gho, M., Bellaïche, Y., and Schweisguth, F. (1999). Revisiting the Drosophila microchaete lineage: A novel intrinsically asymmetric cell division generates a glial cell. Development *126*, 3573–3584.

18. Heitzler, P., and Simpson, P. (1991). The choice of cell fate in the epidermis of Drosophila. Cell *64*, 1083–1092.
19. Lai, E.C. (2004). Notch signaling: Control of cell communication and cell fate. Development *131*, 965–973.
20. Schweisguth, F. (2004). Regulation of notch signaling activity. Curr. Biol. *14*, R129–R138.
21. Simpson, P. (1990). Lateral inhibition and the development of the sensory bristles of the adult peripheral nervous system of Drosophila. Development *109*, 509–519.
22. Huang, F., Dambly-Chaudière, C., and Ghysen, A. (1991). The emergence of sense organs in the wing disc of Drosophila. Development *111*, 1087–1095.
23. Parks, A.L., Huppert, S.S., and Muskavitch, M.A. (1997). The dynamics of neurogenic signalling underlying bristle development in Drosophila melanogaster. Mech. Dev. *63*, 61–74.
24. Hartenstein, V., and Posakony, J.W. (1990). A dual function of the Notch gene in Drosophila sensillum development. Dev. Biol. *142*, 13–30.
25. Usui, K., and Kimura, K. (1993). Sequential emergence of the evenly spaced microchaetes on the notum of Drosophila. Roux's Arch. Dev. Biol. *203*, 151–158.
26. Jhaveri, D., Sen, A., Reddy, G.V., and Rodrigues, V. (2000). Sense organ identity in the Drosophila antenna is specified by the expression of the proneural gene atonal. Mech. Dev. *99*, 101–111.
27. Reddy, G.V., and Rodrigues, V. (1999). A glial cell arises from an additional division within the mechanosensory lineage during development of the microchaete on the Drosophila notum. Development *126*, 4617–4622.
28. Blochlinger, K., Jan, L.Y., and Jan, Y.N. (1993). Postembryonic patterns of expression of cut, a locus regulating sensory organ identity in Drosophila. Development *117*, 441–450.
29. Manning, L., and Doe, C.Q. (1999). Prospero distinguishes sibling cell fate without asymmetric localization in the Drosophila adult external sense organ lineage. Development *126*, 2063–2071.
30. Reddy, G.V., and Rodrigues, V. (1999). Sibling cell fate in the Drosophila adult external sense organ lineage is specified by prospero function, which is regulated by Numb and Notch. Development *126*, 2083–2092.
31. Bellaïche, Y., Gho, M., Kaltschmidt, J.A., Brand, A.H., and Schweisguth, F. (2001). Frizzled regulates localization of cell-fate determinants and mitotic spindle rotation during asymmetric cell division. Nat. Cell Biol. *3*, 50–57.
32. Takemoto, K., Nagai, T., Miyawaki, A., and Miura, M. (2003). Spatiotemporal activation of caspase revealed by indicator that is insensitive to environmental effects. J. Cell Biol. *160*, 235–243.
33. Takemoto, K., Kuranaga, E., Tonoki, A., Nagai, T., Miyawaki, A., and Miura, M. (2007). Local initiation of caspase activation in Drosophila salivary gland programmed cell death in vivo. Proc. Natl. Acad. Sci. USA *104*, 13367–13372.
34. Fichelson, P., and Gho, M. (2003). The glial cell undergoes apoptosis in the microchaete lineage of Drosophila. Development *130*, 123–133.
35. Koto, A., Kuranaga, E., and Miura, M. (2009). Temporal regulation of Drosophila IAP1 determines caspase functions in sensory organ development. J. Cell Biol. *187*, 219–231.
36. Fristrom, D., and Fristrom, J.W. (1993). The metamorphic development of the adult epidermis. In The Development of *Drosophila melanogaster*, *Volume 2*, M. Bate and A. Martinez Arias, eds. (Cold Spring Harbor, NY: Cold Spring Harbor Laboratory Press), pp. 843–897.
37. Siegrist, S.E., Haque, N.S., Chen, C.H., Hay, B.A., and Hariharan, I.K. (2010). Inactivation of both Foxo and reaper promotes long-term adult neurogenesis in Drosophila. Curr. Biol. *20*, 643–648.
38. Barad, O., Rosin, D., Hornstein, E., and Barkai, N. (2010). Error minimization in lateral inhibition circuits. Sci. Signal. *3*, ra51.
39. Cohen, M., Georgiou, M., Stevenson, N.L., Miodownik, M., and Baum, B. (2010). Dynamic filopodia transmit intermittent Delta-Notch signaling to drive pattern refinement during lateral inhibition. Dev. Cell *19*, 78–89.
40. Barolo, S., Castro, B., and Posakony, J.W. (2004). New Drosophila transgenic reporters: Insulated P-element vectors expressing fast-maturing RFP. Biotechniques *36*, 436–440, 442.
41. Castro, B., Barolo, S., Bailey, A.M., and Posakony, J.W. (2005). Lateral inhibition in proneural clusters: cis-regulatory logic and default repression by Suppressor of Hairless. Development *132*, 3333–3344.
42. Welshons, W.J., and Keppy, D.O. (1981). The recombinational analysis of aberrations and the position of the notch locus on the polytene chromosome of Drosophila. Mol. Gen. Genet. *181*, 319–324.
43. Brennan, K., Tateson, R., Lewis, K., and Arias, A.M. (1997). A functional analysis of Notch mutations in Drosophila. Genetics *147*, 177–188.
44. Parody, T.R., and Muskavitch, M.A. (1993). The pleiotropic function of Delta during postembryonic development of Drosophila melanogaster. Genetics *135*, 527–539.
45. Schweisguth, F., and Posakony, J.W. (1992). Suppressor of Hairless, the Drosophila homolog of the mouse recombination signal-binding protein gene, controls sensory organ cell fates. Cell *69*, 1199–1212.
46. Kageyama, R., Ohtsuka, T., Shimojo, H., and Imayoshi, I. (2008). Dynamic Notch signaling in neural progenitor cells and a revised view of lateral inhibition. Nat. Neurosci. *11*, 1247–1251.
47. Shimojo, H., Ohtsuka, T., and Kageyama, R. (2008). Oscillations in notch signaling regulate maintenance of neural progenitors. Neuron *58*, 52–64.
48. Masamizu, Y., Ohtsuka, T., Takashima, Y., Nagahara, H., Takenaka, Y., Yoshikawa, K., Okamura, H., and Kageyama, R. (2006). Real-time imaging of the somite segmentation clock: Revelation of unstable oscillators in the individual presomitic mesoderm cells. Proc. Natl. Acad. Sci. USA *103*, 1313–1318.
49. Doe, C.Q., and Goodman, C.S. (1985). Early events in insect neurogenesis. II. The role of cell interactions and cell lineage in the determination of neuronal precursor cells. Dev. Biol. *111*, 206–219.
50. Brachmann, C.B., and Cagan, R.L. (2003). Patterning the fly eye: The role of apoptosis. Trends Genet. *19*, 91–96.
51. Rusconi, J.C., Hays, R., and Cagan, R.L. (2000). Programmed cell death and patterning in Drosophila. Cell Death Differ. *7*, 1063–1070.
52. Miller, D.T., and Cagan, R.L. (1998). Local induction of patterning and programmed cell death in the developing Drosophila retina. Development *125*, 2327–2335.
53. Cagan, R.L., and Ready, D.F. (1989). Notch is required for successive cell decisions in the developing Drosophila retina. Genes Dev. *3*, 1099–1112.
54. Guo, M., Jan, L.Y., and Jan, Y.N. (1996). Control of daughter cell fates during asymmetric division: Interaction of Numb and Notch. Neuron *17*, 27–41.
55. Buffin, E., and Gho, M. (2010). Laser microdissection of sensory organ precursor cells of Drosophila microchaetes. PLoS ONE *5*, e9285.
56. Orgogozo, V., Schweisguth, F., and Bellaïche, Y. (2002). Binary cell death decision regulated by unequal partitioning of Numb at mitosis. Development *129*, 4677–4684.
57. Werz, C., Lee, T.V., Lee, P.L., Lackey, M., Bolduc, C., Stein, D.S., and Bergmann, A. (2005). Mis-specified cells die by an active gene-directed process, and inhibition of this death results in cell fate transformation in Drosophila. Development *132*, 5343–5352.
58. Avery, L., and Horvitz, H.R. (1987). A cell that dies during wild-type C. elegans development can function as a neuron in a ced-3 mutant. Cell *51*, 1071–1078.
59. Lundell, M.J., Lee, H.K., Pérez, E., and Chadwell, L. (2003). The regulation of apoptosis by Numb/Notch signaling in the serotonin lineage of Drosophila. Development *130*, 4109–4121.
60. Degterev, A., Hitomi, J., Germscheid, M., Ch'en, I.L., Korkina, O., Teng, X., Abbott, D., Cuny, G.D., Yuan, C., Wagner, G., et al. (2008). Identification of RIP1 kinase as a specific cellular target of necrostatins. Nat. Chem. Biol. *4*, 313–321.
61. Golstein, P., and Kroemer, G. (2005). Redundant cell death mechanisms as relics and backups. Cell Death Differ. *12* (*Suppl 2*), 1490–1496.
62. Hay, B.A., Wolff, T., and Rubin, G.M. (1994). Expression of baculovirus P35 prevents cell death in Drosophila. Development *120*, 2121–2129.